DE GRUYTER

Chemical Papers 69 (11) 1421–1437 (2015)
DOI: 10.1515/chempap-2015-0168

ORIGINAL PAPER

Ce(III) immobilised on aminated epichlorohydrin-activated agarose matrix – "green" and efficient catalyst for transamidation of carboxamides

Zeinab Zarei, Batool Akhlaghinia*

Department of Chemistry, Faculty of Sciences, Ferdowsi University of Mashhad, P.O. Box 9177948974, Mashhad, Iran

Received 25 February 2015; Revised 31 May 2015; Accepted 10 June 2015

The present study reports the preparation and characterisation of Ce(III) immobilised on an aminated epichlorohydrin-activated agarose matrix (CAEA) as a "green" catalyst. The catalyst was synthesised by the reaction of the epichlorohydrin-activated agarose matrix with ammonia solution, which was then treated with $Ce(NO_3)_3 \cdot 6H_2O$. The catalyst (CAEA) was characterised by FT-IR, far IR, CHN, XRD, TGA, and ICP techniques. CAEA is shown to be an effective and reusable heterogeneous catalyst for the transamidation of carboxamides with amines under solvent-free conditions. The catalyst was successfully applied to the synthesis of a wide range of aromatic and aliphatic amides. High efficiency, mild reaction conditions, easy work-up, simple separation and also reusability are important advantages of this catalyst.

Keywords: cerium(III) immobilised on aminated epichlorohydrin-activated agarose matrix (CAEA), carboxamides, transamidation, amines

Introduction

Out of the vast array of useful molecules, such as industrially and biologically active compounds including pharmaceuticals and agrochemicals, the amides are prevalent. Hence, there has been increased interest in the synthesis of carboxamides. Formation of the amide linkage has usually been performed by the reaction of amines with carboxylic acid derivatives (chlorides, anhydrides, esters, or acids), alcohols or aldehydes, as well as by the direct amidation of alcohols with nitroarenes, the aminocarbonylation of aryl halides and alkynes, the umpolung reaction of amines with α-halo nitro alkanes, the Beckmann rearrangement, and the cross-coupling of formamides with alkyl/aryl halides (Lundberg et al., 2014). To make use of the low cost and the available starting materials such as amines and amides, transamidation is rapidly acquiring prominence. On the other hand, transamidation is a fairly unusual reaction due to the presence of an acidic N—H bond and, also, the intrinsic strength of the amide C—N bond. In comparison with other acyl derivatives, amides are relatively inert, hence transamidation may be performed under forced reaction conditions, such as using stoichiometric amounts of reagents, high temperature (> 250 °C), and long reaction times.

Transamidation in the presence of an enzyme with a limited range of substrates and requiring long reaction times has also been reported (Sergeeva et al., 2000). To overcome these drawbacks, new homogeneous (Stephenson et al., 2009; Hoerter et al., 2008; Rao et al., 2013; Zhang et al., 2012; Allen et al., 2012; Atkinson et al., 2012; Becerra-Figueroa et al., 2014) and heterogeneous catalysts (Tamura et al., 2012; Wang et al., 2014a) including niobium oxide, cerium dioxide, manganese(II) complex, iron(III), ionic liquid, and sulphuric acid immobilised on silica gel have recently been reported for the transamidation reaction (Ghosh et al., 2014; Singh et al., 2014; Ayub Ali et al., 2014; Fu et al., 2014; Rasheed et al., 2015). The need to use a solvent, followed by difficulties in

*Corresponding author, e-mail: akhlaghinia@um.ac.ir

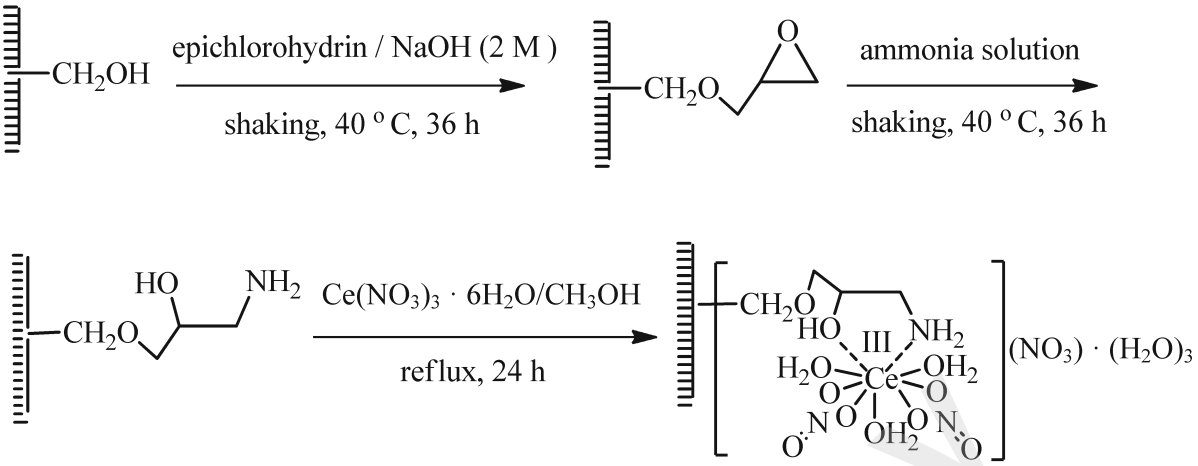

Fig. 1. Preparation of Ce(III) immobilised on aminated epichlorohydrin-activated agarose matrix (CAEA).

the separation and recycling of the catalysts used are disadvantages posed by homogeneous catalysts which are overcome by using heterogeneous catalysts in the transamidation reaction. Many of the protocols referred to above suffer from some disadvantages like the use of expensive reagents, low yields, long reaction times, water sensitivity, tedious work-ups, and difficulty in the separation and the recovery of the catalyst. In view of the increasing demands for organic syntheses, the development of a new, simple, fast, efficient, and highly profitable catalytic transamidation of carboxamides with amines under mild reaction conditions remains highly desirable and in demand.

Following a recent study in the preparation and use of heterogeneous catalysts in organic reactions (Razavi & Akhlaghinia, 2015) and considering that agarose (as a "green", biodegradable and mechanically stable polymer (Wu et al., 2009; Rhim, 2012)) which is widely found in nature has been an ideal candidate for numerous practices in different areas of science, another heterogenous catalyst based on agarose was synthesised, characterised and applied in the transamidation reaction.

Agarose is a linear polymer made up of D-galactose and 3,6-anhydro-L-galactopyranose units. This polysaccharide has properties such as flexibility, non-toxicity, low cost, solubility in hot water, carrying freely available hydroxyl groups to form hydrogen bonds. In the present study, the washed and suction-dried agarose was treated with epichlorohydrin in an alkaline solution incubated with shaking at 40 °C. The resulting epoxy-activated agarose (*I*) was then treated with ammonia solution. To obtain Ce(III) immobilised on the aminated epichlorohydrin-activated agarose matrix (CAEA) (*III*), the aminated epichlorohydrin-activated agarose matrix (*II*) which was used as the support and ligand for entrapment of Ce(III) reacted with a solution of $Ce(NO_3)_3 \cdot 6H_2O$ (Fig. 1).

Experimental

The purity determinations of the products were accomplished by thin layer chromatography (preparative TLC were carried out using a Merck GF 254 silica gel on a glass support). The melting points of products were determined using an Electrothermal Type 9100 melting point apparatus. The FT-IR spectra were recorded on an Avatar 370 FT-IR Thermo Nicolet spectrometer (USA). The far IR spectra in the region 600–300 cm^{-1} were obtained using a Thermo Nicolet NEXUS 870 FT-IR spectrometer (USA) equipped with DTGS/polyethylene detector and a solid substrate beam splitter. The spectra were collected with a resolution of 4 cm^{-1}. NMR spectra were recorded using Bruker Avance 600, Bruker Avance 500, Bruker Avance 400, Bruker DRX 400, Varian Inova 400 and Varian mercury 300 spectrometers (Germany) in $CDCl_3$. Mass spectra 70 eV were recorded using a CH7A Varianmat Bremem instrument (Germany). Elemental analysis were performed using a Costech 4010 CHNS Elemental Analyser instrument (Italy). Thermogravimetric analysis (TGA) was performed on a Shimadzu Thermogavimetric Analyser (TG-50, Switzerland) under an air atmosphere, with a heating rate of 10 °C min^{-1}. Inductively-coupled plasma (ICP) measurements were carried out on a Varian, VISTA-PRO, CCD (Australia). Most of the products were known compounds characterised by FT-IR, NMR spectroscopy, mass spectrometry, and by comparing their melting points with the melting points of known compounds. The commercially available agarose was washed as previously reported in the literature (Cao et al., 1997).

Matrices preparation

Washed and suction-dried agarose (2 g) was added to 8 mL of distilled water and mixed with 10 mL of

Table 1. Characterisation data of newly prepared amide (*N*-(3-ethoxypropyl)benzamide)

Entry	Compound	M_r	w_i(calc.)/mass % w_i(found)/mass %			Isolated yield	M.p.
			C	H	N	%	℃
26	$C_{12}H_{17}NO_2$	207	69.54 69.34	8.27 8.28	6.76 6.78	80	(oil)

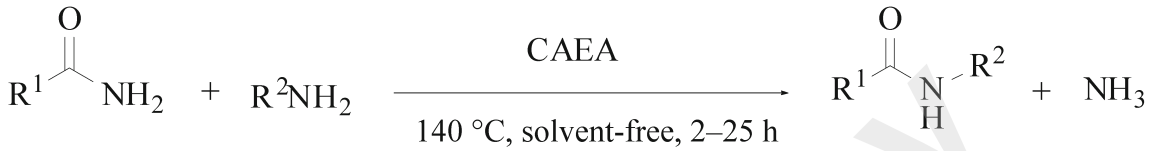

R^1 = phenyl, 4-methoxyphenyl, 3,4-dimethylphenyl, 4-methylphenyl, 4-bromophenyl, 2-chlorophenyl, 3,4-dichlorophenyl, 3-nitrophenyl, 4-nitrophenyl, pyridyl, cinnamyl, 4-chlorocinnamyl, 3-nitrocinnamyl, 2,4-dichloro-1-methoxyphenyl, diphenylmethyl, heptadec-8-enyl, hexyl

R^2 = benzyl, 4-methoxybenzyl, 2-chlorobenzyl, benzene, 4-methoxybenzene, 3,4-dimethylbenzene, 4-methylbenzene, furan-2-ylmethyl, cyclohexyl, butyl, 3-ethoxypropyl, piperidine, morpholine, pyrrolidine

Fig. 2. Transamidation of various amides with various amines in the presence of Ce(III) immobilised on aminated epichlorohydrin-activated agarose matrix (CAEA).

NaOH (2 mol L^{-1}) at ambient temperature. Epichlorohydrin (6 mL) was added to the resulting suspension and incubated at 40 ℃ with shaking. After 36 h, the suspension was cooled to ambient temperature, filtered, and washed with distilled water (4 × 15 mL) to remove the surplus amount of epichlorohydrin. The epoxy-activated agarose (*I*) was dried at ambient temperature (1.80 g, 76 %).

The epoxy-activated agarose (1.80 g) was added to a concentrated ammonia solution (20 mL) incubated at 40 ℃ with shaking. After 36 h, the resulting suspension was cooled to ambient temperature and filtered. The resulting gel was washed with water (4 × 15 mL), brine (3 × 5 mL), and water (4 × 15 mL) until the filtrate was neutral. The aminated epichlorohydrin-activated agarose matrix (*II*) was dried at ambient temperature.

To a solution of $Ce(NO_3)_3 \cdot 6H_2O$ (1 mmol, 0.43 g) in CH_3OH (10 mL), aminated epichlorohydrin-activated agarose matrix (*II*) (0.37 g) was added. The reaction mixture was refluxed for 24 h and then allowed to cool to ambient temperature. The Ce(III) immobilised on aminated epichlorohydrin-activated agarose matrix CAEA (*III*) (0.47 g, 70 %) as a pale yellow precipitate was filtered, washed with CH_3OH, and dried at ambient temperature.

General procedure for transamidation of benzamide with benzylamine using CAEA and recovery of CAEA

CAEA (0.01 g) was added to a mixture of benzamide (1 mmol, 0.121 g) and benzylamine (1.1 mmol, 0.117 g) in a round-bottom flask equipped with a condenser under solvent-free conditions. The reaction mixture was stirred (250 min^{-1}) at 140 ℃. The progress of the reaction was monitored by TLC. Following the reaction, the reaction mixture was cooled and the resultant mixture was submitted to silica gel preparative TLC using ethyl acetate/hexane (1/1) as eluent. *N*-Benzylbenzamide was obtained with a 95 % yield (0.198 g). The spectral data of the compounds are given in Tables 1 and 2.

The reaction mixture was centrifuged (1000 min^{-1}, 10 min) and washed several times with ethyl acetate and acetone to remove all the organic compounds then the precipitate was dried at ambient temperature.

Results and discussion

In continuing efforts to develop efficient and environmentally benign amide formation methods (Ghodsinia et al., 2013), it was envisioned that CAEA as a "green" catalyst could effectively catalyse the transamidation of various primary amides with various primary and secondary amines to afford the corresponding *N*-alkylamides with high yields at 140 ℃ under solvent-free conditions (Fig. 2).

First, the transamidation reaction between benzamide and benzylamine was examined in the presence of CAEA under various reaction conditions (Table 3). There was hardly any transamidation without a catalyst (Table 3, entry 1). In the presence of CAEA (0.01 g, 1.61 mole %, of CAEA contains 0.002 g, 0.01 mmol, of Ce), the desired product was obtained with a low yield (Table 3, entry 2). To increase the con-

Table 2. Characterisation data of prepared amides

Entry	Characterisation data
1	*N*-Benzylbenzamide White solid IR, $\tilde{\nu}$/cm^{-1}: 3291 (NH), 3063 (Ph), 1638 (C═O) ^{1}H NMR (400 MHz, $CDCl_3$), δ: 7.81 (d, 2H, $^3J_{HH}$ = 8 Hz, Ph), 7.55–7.51 (m, 1H, Ph), 7.46 (t, 2H, $^3J_{HH}$ = 8 Hz, Ph), 7.39–7.29 (m, 5H, Ph), 6.47 (brs, 1H, NH) D_2O exchangeable, 4.67 (d, 2H, $^3J_{HH}$ = 5.6 Hz, CH_2) ^{13}C NMR (125 MHz, $CDCl_3$), δ: 167.3 (CO), 138.2, 134.3, 131.3, 128.6, 128.4, 127.7, 127.4, 126.9, 43.9 (CH_2) MS, m/z (I_r/%): 211 (8) (M^+), 106 (20) ($PhCH_2NH$), 104 (100) (PhCO), 90 (70) ($PhCH_2$), 76 (88) (Ph)
2	*N*-Benzyl-4-methoxybenzamide Yellow solid IR, $\tilde{\nu}$/cm^{-1}: 3266 (NH), 3051 (Ph), 1632 (C═O) ^{1}H NMR (400 MHz, $CDCl_3$), δ: 7.76 (d, 2H, $^3J_{HH}$ = 8 Hz, Ph), 7.36–7.30 (m, 5H, Ph), 6.92 (d, 2H, $^3J_{HH}$ = 8 Hz, Ph), 6.91 (brs, 1H, NH) D_2O exchangeable, 4.62 (d, 2H, $^3J_{HH}$ = 5.6 Hz, CH_2), 3.84 (s, 3H, OCH_3) ^{13}C NMR (125 MHz, $CDCl_3$), δ: 166.9 (CO), 162.1, 138.4, 128.7, 128.5, 127.7, 127.3, 126.6, 113.6, 55.2 (CH_3), 43.8 (CH_2) MS, m/z (I_r/%): 241 (18) (M^+), 134 (100) (M^+ – $PhCH_2NH$), 106 (71) ($PhCH_2NH$), 91 (73) ($PhCH_2$), 76 (75) (Ph), 28 (64) (CO)
3	*N*-Benzyl-3,5-dimethylbenzamide Colourless solid IR, $\tilde{\nu}$/cm^{-1}: 3237 (NH), 3064 (Ph), 3019 (Ph), 1643 (C═O) ^{1}H NMR (400 MHz, $CDCl_3$), δ: 7.42 (s, 2H, Ph), 7.40–7.38 (m, 4H, Ph), 7.36–7.31 (m, 1H, Ph), 7.16 (s, 1H, Ph), 6.38 (brs, 1H, NH) D_2O exchangeable, 4.67 (d, 2H, $^3J_{HH}$ = 5.6 Hz, CH_2), 2.37 (s, 6H, 2Me) ^{13}C NMR (125 MHz, $CDCl_3$), δ: 167.8 (CO), 138.3, 134.4, 133.2, 128.8, 127.9, 127.6, 124.7, 44.1 (CH_2), 21.2 (CH_3) MS, m/z (I_r/%): 239 (90) (M^+), 133 (95) (M^+ – $PhCH_2NH$), 105 (85) ($PhCH_2NH$), 91 (35) ($PhCH_2$), 77 (20) (Ph)
4	*N*-Benzyl-4-methylbenzamide Yellow solid IR, $\tilde{\nu}$/cm^{-1}: 3310 (NH), 3058 (Ph), 3027 (Ph), 1640 (C═O) ^{1}H NMR (400 MHz, $CDCl_3$), δ: 7.68 (d, 2H, $^3J_{HH}$ = 8 Hz, Ph), 7.37–7.30 (m, 5H, Ph), 7.23 (d, 2H, $^3J_{HH}$ = 8 Hz, Ph), 6.42 (brs, 1H, NH) D_2O exchangeable, 4.63 (d, 2H, $^3J_{HH}$ = 5.6 Hz, CH_2), 2.39 (s, 3H, Me) ^{13}C NMR (125 MHz, $CDCl_3$), δ: 167.2 (CO), 141.8, 138.3, 131.5, 129.1, 128.6, 127.8, 127.4, 126.9, 44.0 (CH_2), 21.3 (CH_3) MS, m/z (I_r/%): 211 (8) (M^+), 105 (100) ($PhCH_2NH$), 91 (63) ($PhCH_2$), 77 (92) (Ph), 28 (87) (CO)
5	*N*-Benzyl-4-bromobenzamide White solid IR, $\tilde{\nu}$/cm^{-1}: 3312 (NH), 3055 (Ph), 3022 (Ph), 1640 (C═O) ^{1}H NMR (400 MHz, $CDCl_3$), δ: 7.64 (d, 2H, $^3J_{HH}$ = 8.8 Hz, Ph), 7.53 (d, 2H, $^3J_{HH}$ = 8.8 Hz, Ph), 7.35–7.30 (m, 5H, Ph), 6.70 (brs, 1H, NH) D_2O exchangeable, 4.60 (d, 2H, $^3J_{HH}$ = 5.6 Hz, CH_2) ^{13}C NMR (125 MHz, $CDCl_3$), δ: 166.3 (CO), 137.9, 137.7, 132.7, 128.7, 128.4, 127.8, 127.6, 44.1 (CH_2) MS, m/z (I_r/%): 210 (5) (M^+ – Br), 119 (98) (PhCONH), 106 (70) ($PhCH_2NH$), 91 (85) ($PhCH_2$), 77 (62) (Ph), 28 (80) (CO)
6	*N*-Benzyl-2-chlorobenzamide Yellow solid IR, $\tilde{\nu}$/cm^{-1}: 3257 (NH), 3087 (Ph), 3027 (Ph), 2917 (CH_2), 1637 (C═O) ^{1}H NMR (400 MHz, $CDCl_3$), δ: 7.71–7.69 (m, 4H, Ph), 7.38–7.31 (m, 5H, Ph), 6.49 (brs, 1H, NH) D_2O exchangeable, 4.68 (d, 2H, $^3J_{HH}$= 5.6 Hz, CH_2) ^{13}C NMR (125 MHz, $CDCl_3$), δ: 167.3 (CO), 135.5, 134.2, 133.5, 131.5, 130.1, 129.4, 128.8, 128.5, 127.0, 126.9, 41.9 (CH_2) MS, m/z (I_r/%): 246 (18) (M^+), 208 (97) (M^+ – Cl), 138 (100) (M^+ – $PhCH_2NH$), 91 (44) ($PhCH_2$), 28 (64) (CO)
7	*N*-Benzyl-3,4-dichlorobenzamide Light orange solid IR, $\tilde{\nu}$/cm^{-1}: 3320 (NH), 3080 (Ph), 3027 (Ph), 2921 (CH_2), 2851 (CH_2), 1643 (C═O) ^{1}H NMR (400 MHz, $CDCl_3$), δ: 7.91 (d, 1H, $^4J_{HH}$ = 1.6 Hz, Ph), 7.64–7.62 (m, 1H, Ph), 7.52 (d, 1H, $^3J_{HH}$ = 8 Hz, Ph), 7.41–7.29 (m, 5H, Ph), 6.47 (brs, 1H, NH) D_2O exchangeable, 4.64 (d, 2H, $^3J_{HH}$= 5.6 Hz, CH_2) ^{13}C NMR (125 MHz, $CDCl_3$), δ: 165.2 (CO), 137.6, 135.9, 134.1, 133.0, 130.6, 129.1, 128.8, 127.8, 127.7, 126.1, 44.3 (CH_2) MS, m/z (I_r/%): 279 (35) (M^+), 172 (100) (M^+ – $PhCH_2NH$), 144 (95) (M^+ – $PhCH_2NHCO$), 106 (98) ($PhCH_2NH$), 90 (89) ($PhCH_2$), 77 (70) (Ph)

Table 2. (continued)

Entry	Characterisation data
8	*N*-Benzyl-3-nitrobenzamide Yellow solid IR, $\tilde{\nu}$/cm^{-1}: 3295 (NH), 3084 (Ph), 3031(Ph), 2917 (CH_2), 1642 (C═O), 1351 (NO_2) ^{1}H NMR (400 MHz, $CDCl_3$), δ: 8.61 (s, 1H, Ph), 8.36 (d, 1H, $^3J_{HH}$ = 6.4 Hz, Ph), 8.18 (d, 2H, $^3J_{HH}$ = 8 Hz, Ph), 7.65 (d, 2H, $^3J_{HH}$ = 8 Hz, Ph), 7.37–7.26 (m, 3H, Ph), 6.69 (brs, 1H, NH) D_2O exchangeable, 4.67 (s, 2H, CH_2) ^{13}C NMR (125 MHz, $CDCl_3$), δ: 166.0 (CO), 137.8, 136.2, 134.3, 130.1, 130.0, 128.6, 127.7, 127.5, 125.5, 122.6, 44.0 (CH_2) MS, m/z (I_r/%): 258 (12) (M^+), 207 (20) ($M^+ - NO_2$), 149 (92) ($M^+ - PhCH_2NH$), 104 (92) ($PhCH_2NH$), 91 (63) ($PhCH_2$), 77 (67) (Ph), 29 (72) (CO)
9	*N*-Benzyl-4-nitrobenzamide Yellow solid IR, $\tilde{\nu}$/cm^{-1}: 3279 (NH), 3031(Ph), 1630 (C═O), 1536 (NO_2), 1346 (NO_2) ^{1}H NMR (400 MHz, $CDCl_3$), δ: 8.26 (d, 2H, $^3J_{HH}$ = 8.8 Hz, Ph), 7.94 (d, 2H, $^3J_{HH}$ = 8.8 Hz, Ph), 7.38–7.34 (m, 5H, Ph), 7.26 (brs, 1H, NH) D_2O exchangeable, 4.65 (d, 2H, $^3J_{HH}$ = 5.6 Hz, CH_2) ^{13}C NMR (125 MHz, $CDCl_3$), δ: 165.4 (CO), 149.5, 139.8, 137.4, 128.8, 128.2, 127.8, 123.7, 44.3 (CH_2) MS, m/z (I_r/%): 256 (12) (M^+), 207 (20) ($M^+ - NO_2$), 149 (92) ($M^+ - PhCH_2NH$), 104 (92) ($PhCH_2NH$), 91 (75) ($PhCH_2$), 77 (78) (Ph), 29 (72) (CO)
10	*N*-Benzylisonicotinamide White solid IR, $\tilde{\nu}$/cm^{-1}: 3313 (NH), 3060 (Ph), 3027 (Ph), 2880 (CH_2), 1648 (C═O) ^{1}H NMR (400 MHz, $CDCl_3$), δ: 8.91 (d, 2H, $^3J_{HH}$ = 4.4 Hz, pyridine ring), 7.77 (d, 2H, $^3J_{HH}$ = 4.4 Hz, pyridine ring), 7.45–7.29 (m, 5H, Ph), 6.95 (brs, 1H, NH) D_2O exchangeable, 4.64 (d, 2H, $^3J_{HH}$ = 5.2 Hz, CH_2) ^{13}C NMR (125 MHz, $CDCl_3$), δ: 165.6 (CO), 150.4, 141.3, 137.5, 128.9, 128.0, 127.7, 122.0, 44.3 (CH_2) MS, m/z (I_r/%): 212 (48) (M^+), 106 (27) ($PhCH_2NH$), 78 (13) ($M^+ - PhCH_2NHCO$), 57 (27) (CH_2NHCO), 29 (94) (CO)
11	*N*-Benzylcinnamamide White solid IR, $\tilde{\nu}$/cm^{-1}: 3280 (NH), 3080 (Ph), 3031(Ph), 2917 (CH_2), 1613 (C═O) ^{1}H NMR (400 MHz, $CDCl_3$), δ: 7.63 (d, 1H, $^3J_{HH}$ = 15.6 Hz, CH=), 7.43 (dd, 2H, $^{3,4}J_{HH}$ = 6.4 Hz, 2.8 Hz, Ph), 7.35–7.32 (m, 8H, Ph), 6.52 (brs, 1H, NH) D_2O exchangeable, 6.45 (d, 1H, $^3J_{HH}$ = 15.6 Hz, CH=), 4.50 (d, 2H, $^3J_{HH}$ = 5.8 Hz, CH_2) ^{13}C NMR (125 MHz, $CDCl_3$), δ: 166.1 (CO), 141.3, 138.4, 134.0, 128.9, 128.1, 127.9, 127.6, 120.8, 43.9 (CH_2) MS, m/z (I_r/%): 237 (40) (M^+), 130 (100) ($M^+ - PhCH_2NH$), 106 (95) ($PhCH_2NH$), 91 (72) ($PhCH_2$), 77 (95) (Ph), 28 (75) (CO)
12	(*E*)-*N*-Benzyl-3-(4-chlorophenyl)acrylamide White solid IR, $\tilde{\nu}$/cm^{-1}: 3288 (NH), 3064 (Ph), 2929 (CH_2), 1622 (C═O) ^{1}H NMR (400 MHz, $CDCl_3$), δ: 7.65 (d, 1H, $^3J_{HH}$ = 15.6 Hz, CH=), 7.42–7.40 (m, 4H, Ph), 7.38–7.29 (m, 5H, Ph), 6.49 (d, 1H, $^3J_{HH}$ = 15.6 Hz, CH=), 6.24 (brs, 1H, NH) D_2O exchangeable, 4.60 (d, 2H, $^3J_{HH}$ = 4.4 Hz, CH_2) ^{13}C NMR (125 MHz, $CDCl_3$), δ: 165.6 (CO), 140.1, 138.1, 135.6, 133.3, 129.1, 129.0, 128.8, 127.9, 127.6, 121.0, 43.9 (CH_2) MS, m/z (I_r/%): 273 (15) ($M^+ + 2$), 271 (45) (M^+), 164 (98) ($M^+ - PhCH_2NH$), 106 (85) ($PhCH_2NH$), 90 (25) ($PhCH_2$)
13	(*E*)-*N*-Benzyl-3-(3-nitrophenyl)acrylamide Yellow solid IR, $\tilde{\nu}$/cm^{-1}: 3223 (NH), 3069 (Ph), 1656 (C═O), 1530 (NO_2), 1347 (NO_2) ^{1}H NMR (400 MHz, $CDCl_3$), δ: 8.31 (s, 1H, Ph), 8.15 (d, 1H, $^3J_{HH}$ = 8.2 Hz, Ph), 7.71 (d, 1H, $^3J_{HH}$ = 7.7 Hz, Ph), 7.66 (d, 1H, $^3J_{HH}$ = 15.6 Hz, CH=), 7.52 (t, 1H, $^3J_{HH}$ = 8.2 Hz, Ph), 7.34–7.24 (m, 5H, Ph), 6.60 (d, 1H, $^3J_{HH}$ = 15.6 Hz, CH=), 6.48 (brs, 1H, NH) D_2O exchangeable, 4.57 (d, 2H, $^3J_{HH}$ = 5.8 Hz, CH_2) ^{13}C NMR (125 MHz, $CDCl_3$), δ: 165.1 (CO), 148.7, 138.8, 138.0, 136.7, 134.1, 130.0, 128.9, 128.0, 127.8, 124.1, 123.7, 121.8, 44.8 (CH_2) MS, m/z (I_r/%): 282 (5) (M^+), 175 (25) ($M^+ - PhCH_2NH$), 160 (60) ($M^+ - PhNO_2$), 106 (65) ($PhCH_2NH$), 91 (50) ($PhCH_2$), 77 (22) (Ph), 28 (100) (CO)
14	*N*-Benzyl-2-(2,4-dichlorophenoxy)acetamide Yellow–brown oily liquid IR, $\tilde{\nu}$/cm^{-1}: 3287 (NH), 3096 (Ph), 3035 (Ph), 2933 (CH_2), 2855 (CH_2), 1661 (C═O) ^{1}H NMR (400 MHz, $CDCl_3$), δ: 7.39–7.34 (m, 5H, Ph), 7.23–7.21 (m, 1H, Ph), 7.10 (brs, 1H, NH) D_2O exchangeable, 6.83–6.85 (m, 2H, Ph), 4.57–4.58 (m, 4H, CH_2) MS, m/z (I_r/%): 309 (15) (M^+), 174 (8) ($M^+ - PhCH_2NHCO$), 147 (100) ($PhCH_2NHCOCH_2$), 107 (47) ($PhCH_2NH$), 91 (99) ($PhCH_2$), 28 (68) (CO)

Table 2. (continued)

Entry	Characterisation data
15	*N*-Benzyl-2,2-diphenylacetamide Yellow solid IR, $\tilde{\nu}$/cm^{-1}: 3311 (NH), 3064 (Ph), 3031(Ph), 2933 (CH_2), 1641 (C═O) ^{1}H NMR (400 MHz, $CDCl_3$), δ: 7.33–7.31 (m, 5H, Ph), 7.28–7.20 (m, 10H, 2Ph), 5.91 (brs, 1H, NH) D_2O exchangeable, 4.97 (s, 1H, CH), 4.50 (d, 2H, $^3J_{HH}$ = 5.6 Hz, CH_2) ^{13}C NMR (125 MHz, $CDCl_3$), δ: 171.8 (CO), 139.4, 138.1, 128.9, 128.8, 128.7, 127.7, 127.5, 127.3, 59.2 (CH), 43.8 (CH_2) MS, m/z (I_r/%): 301 (88) (M^+), 167 (100) ($CH(Ph)_2$), 91 (52) ($PhCH_2$)
16	*N*-Benzyloleamide Light yellow oil IR, $\tilde{\nu}$/cm^{-1}: 3302 (NH), 2921 (CH_2), 2850 (CH_2), 1640 (C═O) ^{1}H NMR (400 MHz, $CDCl_3$), δ: 7.33–7.28 (m, 5H, Ph), 5.76 (brs, 1H, NH) D_2O exchangeable, 5.34 (s, 2H, CH_2), 4.44 (d, 2H, $^3J_{HH}$ = 5.2 Hz, CH_2), 2.22–2.18 (d, 2H, $^3J_{HH}$ = 15.2 Hz, CH=), 2.01 (s, 3H), 1.66 (s, 4H), 1.29–1.27 (m, 14H), 0.89–0.87 (m, 8H) MS, m/z (I_r/%): 371 (11) (M^+), 162 (23) ($PhCH_2NHCO(CH_2)_2$), 149 (83) ($PhCH_2NHCOCH_2$), 106 (76) ($PhCH_2NH$), 91 (100) ($PhCH_2$), 43 (65) (CONH), 28 (52) (CO)
17	*N*-(4-Methoxybenzyl)benzamide White solid IR, $\tilde{\nu}$/cm^{-1}: 3245 (NH), 3080 (Ph), 2929 (CH_2), 1633 (C═O) ^{1}H NMR (400 MHz, $CDCl_3$), δ: 7.79–7.77 (d, 2H, $^3J_{HH}$ = 8 Hz, Ph), 7.50–7.48 (d, 2H, $^3J_{HH}$ = 8 Hz, Ph), 7.44–7.43 (m, 1H, Ph), 7.30–7.28 (d, 2H, $^3J_{HH}$ = 8 Hz, Ph), 6.90–6.88 (d, 2H, $^3J_{HH}$ = 8 Hz, Ph), 6.35 (brs, 1H, NH) D_2O exchangeable, 4.59 (s, 2H, CH_2), 3.81 (s, 3H, OCH_3) ^{13}C NMR (125 MHz, $CDCl_3$), δ: 167.2 (CO), 159.0, 134.4, 131.3, 130.3, 129.1, 128.4, 126.9, 114.0, 55.2 (C), 43.5 (CH_2) MS, m/z (I_r/%): 241 (5) (M^+), 135 (70) (M^+ – PhCO), 120 (80) (PhCONH), 104 (100) ($PhCH_2NH$), 76 (82) (Ph), 28 (97) (CO)
18	*N*-(2-Chlorobenzyl)benzamide Light yellow solid IR, $\tilde{\nu}$/cm^{-1}: 3287 (NH), 3062 (Ph), 3023 (Ph), 1632 (C═O) ^{1}H NMR (400 MHz, $CDCl_3$), δ: 7.78 (d, 2H, $^3J_{HH}$ = 8 Hz, Ph), 7.51–7.45 (m, 1H, Ph), 7.41–7.36 (m, 4H, Ph), 7.26–7.22 (m, 2H, Ph), 6.77 (brs, 1H, NH) D_2O exchangeable, 4.70 (d, 2H, $^3J_{HH}$ = 5.6 Hz, CH_2) ^{13}C NMR (125 MHz, $CDCl_3$), δ: 167.4 (CO), 131.6, 130.3, 129.5, 129.0, 128.6, 127.1, 127.0, 41.0 (CH_2) MS, m/z (I_r/%): 225 (8) (M^+), 209 (32) (M^+ – Cl), 105 (100) (PhCO), 91 (64) ($PhCH_2$), 77 (91) (Ph), 28 (86) (CO)
19	*N*-Phenylbenzamide Colourless solid IR, $\tilde{\nu}$/cm^{-1}: 3345 (NH), 3056 (Ph), 1655 (C═O) ^{1}H NMR (400 MHz, $CDCl_3$), δ: 8.00 (brs, 1H, NH) D_2O exchangeable, 7.87 (d, 2H, $^3J_{HH}$ = 8 Hz, Ph), 7.65 (d, 2H, $^3J_{HH}$ = 8 Hz, Ph), 7.55–7.53 (m, 1H, Ph), 7.47 (t, 2H, $^3J_{HH}$ = 8 Hz, Ph), 7.37 (t, 2H, $^3J_{HH}$ = 8 Hz, Ph), 7.16 (t, 1H, $^3J_{HH}$ = 8 Hz, Ph) ^{13}C NMR (125 MHz, $CDCl_3$), δ: 165.8 (CO), 137.9, 135.0, 131.7, 129.0, 128.7, 127.0, 124.5, 120.2 MS, m/z (I_r/%): 197 (11) (M^+), 105 (100) (PhCO), 92 (14) (PhNH), 29 (35) (CO)
20	*N*-(4-Methoxyphenyl)benzamide Colourless solid IR, $\tilde{\nu}$/cm^{-1}: 3329 (NH), 2955 (Ph), 1642 (C═O) ^{1}H NMR (400 MHz, $CDCl_3$), δ: 7.91 (brs, 1H, NH) D_2O exchangeable, 7.87 (d, 2H, $^3J_{HH}$ = 8 Hz, Ph), 7.56–7.52 (m, 3H, Ph), 7.48–7.45 (m, 2H, Ph), 6.89 (d, 2H, $^3J_{HH}$ = 8 Hz, Ph), 3.81 (s, 3H, OMe) ^{13}C NMR (125 MHz, $CDCl_3$), δ: 165.6 (CO), 156.6, 135.0, 131.6, 131.0, 128.6, 126.9, 122.1, 114.2, 55.4 (CH_3) MS, m/z (I_r/%): 227 (13) (M^+), 121 (54) (M^+ – PhCO), 104 (100) (PhCO), 76 (82) (Ph), 28 (66) (CO)
21	*N*-(3,4-Dimethylphenyl)benzamide Colourless solid IR, $\tilde{\nu}$/cm^{-1}: 3307 (NH), 3056 (Ph), 1648 (C═O) ^{1}H NMR (400 MHz, $CDCl_3$), δ: 8.23 (brs, 1H, NH) D_2O exchangeable, 7.86 (d, 2H, $^3J_{HH}$ = 8 Hz, Ph), 7.51–7.48 (m, 1H, Ph), 7.45 (s, 1H, Ph), 7.41–7.38 (m, 3H, Ph), 7.07 (d, 1H, $^3J_{HH}$ = 8 Hz, Ph), 2.24 (s, 3H, Me), 2.22 (s, 3H, Me) ^{13}C NMR (125 MHz, $CDCl_3$), δ: 165.8 (CO), 137.0, 135.6, 134.9, 132.7, 131.4, 129.8, 128.4, 127.0, 121.8, 118.0, 19.6 (CH_3), 19.0 (CH_3) MS, m/z (I_r/%): 225 (21) (M^+), 121 (7) (M^+ – PhCO), 105 (100) (PhCO), 77 (94) (Ph), 29 (68) (CO)

Table 2. (continued)

Entry	Characterisation data
22	*N-(p*-Tolyl)benzamide Colourless solid IR, $\tilde{\nu}$/cm^{-1}: 3310 (NH), 3072 (Ph), 1647 (C═O) ^{1}H NMR (400 MHz, $CDCl_3$), δ: 7.87 (d, 2H, $^3J_{HH}$ = 8 Hz, Ph), 7.70 (brs, 1H, NH) D_2O exchangeable, 7.56–7.48 (m, 5H, Ph), 7.18 (d, 2H, $^3J_{HH}$ = 8 Hz, Ph), 2.34 (s, 3H, Me) ^{13}C NMR (125 MHz, $CDCl_3$), δ: 165.8 (CO), 135.3, 134.9, 134.0, 131.5, 129.4, 128.5, 127.0, 120.4, 20.8 (CH_3) MS, m/z (I_r/%): 211 (8) (M^+), 106 (20) (M^+ – PhCO), 104 (100) (PhCO), 90 (70) ($PhCH_3$), 76 (90) (Ph)
23	*N*-(Furan-2-ylmethyl)benzamide Light yellow solid IR, $\tilde{\nu}$/cm^{-1}: 3301 (NH), 3080 (Ph), 1641 (C═O) ^{1}H NMR (400 MHz, $CDCl_3$), δ: 7.79 (d, 2H, $^3J_{HH}$ = 8.5 Hz, Ph), 7.50–7.49 (m, 1H, CH, furan ring), 7.43–7.26 (m, 3H, Ph), 6.47 (brs, 1H, NH) D_2O exchangeable, 6.33 (m, 2H, furan ring), 4.64 (d, 2H, $^3J_{HH}$ = 6 Hz, CH_2) ^{13}C NMR (125 MHz, $CDCl_3$), δ: 167.3 (CO), 151.1, 142.2, 134.1, 131.5, 128.5, 127.0, 110.5, 107.6, 36.9 (CH_2) MS, m/z (I_r/%): 201 (29) (M^+), 105 (100) (PhCO), 80 (27) (M^+ – PhCONH), 77 (95) (Ph), 28 (62) (CO)
24	*N*-Cyclohexylbenzamide White solid IR, $\tilde{\nu}$/cm^{-1}: 3241 (NH), 3084 (Ph), 1627 (C═O) ^{1}H NMR (400 MHz, $CDCl_3$), δ: 7.69–7.42 (m, 2H, Ph), 7.42–7.30 (m, 3H, Ph), 6.03 (brs, 1H, NH) D_2O exchangeable, 3.91–3.84 (m, 1H, CH), 1.95–1.92 (m, 2H), 1.68–1.55 (m, 3H), 1.40–1.28 (m, 2H), 1.22–1.09 (m, 3H) ^{13}C NMR (125 MHz, $CDCl_3$), δ: 169.2 (CO), 137.7, 133.8, 131.1, 129.4, 51.3 (CH_2), 35.8 (CH_2), 28.2 (CH_2), 27.5 (CH_2) MS, m/z (I_r/%): 203 (42) (M^+), 121 (98) (PhCONH), 104 (100) (PhCO), 77 (82) (Ph), 28 (89) (CO)
25	*N*-Butylbenzamide Light yellow solid IR, $\tilde{\nu}$/cm^{-1}: 3324 (NH), 3060 (Ph), 2959 (CH_2), 2930 (CH_2), 2872 (CH_2), 1640 (C═O) ^{1}H NMR (400 MHz, $CDCl_3$), δ: 7.76 (d, 2H, $^3J_{HH}$= 8 Hz, Ph), 7.48 (d, 1H, $^3J_{HH}$= 8 Hz, Ph), 7.44–7.43 (m, 2H, Ph), 6.17 (brs, 1H, NH) D_2O exchangeable, 3.49–3.44 (m, 2H, CH_2), 1.62–1.57 (m, 2H, CH_2), 1.44–1.41 (m, 2H, CH_2), 0.98–0.94 (m, 3H, Me) ^{13}C NMR (125 MHz, $CDCl_3$), δ: 167.5 (CO), 134.8, 131.1, 128.4, 126.8, 39.7 (CH_2), 31.6 (CH_2), 20.1 (CH_2), 13.7 (CH_3) MS, m/z (I_r/%): 177 (10) (M^+), 105 (100) (PhCO), 72 (88) (($CH_2)_4$NH), 57 (70) ($CONHCH_2$), 28 (70) (CO)
26	*N*-(3-Ethoxypropyl)benzamide Red wine oil IR, $\tilde{\nu}$/cm^{-1}: 3311 (NH), 3068 (Ph), 2955 (CH_2), 2925 (CH_2), 2868 (CH_2), 1643 (C═O) ^{1}H NMR (400 MHz, $CDCl_3$), δ: 7.77 (d, 2H, $^3J_{HH}$= 8 Hz, Ph), 7.46–7.21 (m, 3H, Ph), 7.21 (brs, 1H, NH) D_2O exchangeable, 3.60–3.49 (m, 4H, 2CH_2), 3.42–3.41 (m, 2H, CH_2), 1.82–1.81 (m, 2H, CH_2), 1.24–1.21 (m, 3H, CH_3) ^{13}C NMR (125 MHz, $CDCl_3$), δ: 167.1 (CO), 134.7, 131.1, 128.4, 126.8, 70.4 (CH_2), 66.5 (CH_2), 39.3 (CH_2), 28.8 (CH_2), 15.3 (CH_3) MS, m/z (I_r/%): 207 (15) (M^+), 178 (5) (M^+ – CH_2CH_3), 162 (20) (M^+ – OCH_2CH_3), 106 (75) (PhCO), 60 (25) ($CH_2OCH_2CH_3$), 28 (58) (CO) Composition for $C_{12}H_{17}NO_2$, w_i/mass %: C 69.54, H 8.27, N 6.76 (calc.); C 69.34, H 8.28, N 6.78 (found)
27	Phenyl(piperidin-1-yl)methanone Colourless oil IR, $\tilde{\nu}$/cm^{-1}: 3058 (Ph), 2998 (CH_2), 2937 (CH_2), 2855 (CH_2), 1629 (C═O) ^{1}H NMR (400 MHz, $CDCl_3$), δ: 7.38–7.37 (m, 5H, Ph), 3.80 (s, 2H, CH_2), 3.68 (s, 2H, CH_2), 1.66–1.40 (m, 6H, 3CH_2) ^{13}C NMR (125 MHz, $CDCl_3$), δ: 170.3 (CO), 136.6, 129.4, 128.4, 126.8, 48.8 (CH_2), 43.1 (CH_2), 25.7 (CH_2), 24.6 (CH_2), 22.6 (CH_2) MS, m/z (I_r/%): 189 (15) (M^+), 105 (100) (PhCO), 86 (70) (M^+ – PhCO), 77 (75) (Ph), 28 (72) (CO)
28	Morpholino(phenyl)methanone Yellow oil IR, $\tilde{\nu}$/cm^{-1}: 3080 (Ph), 2913 (CH_2), 2858 (CH_2), 1626 (C═O) ^{1}H NMR (400 MHz, $CDCl_3$), δ: 7.39–7.26 (m, 5H, Ph), 3.72 (s, 2H, CH_2), 3.35 (s, 2H, CH_2), 1.68 (s, 2H, CH_2), 1.52–1.43 (m, 2H, CH_2) ^{13}C NMR (125 MHz, $CDCl_3$), δ: 170.5 (CO), 135.3, 129.9, 128.6, 128.6, 128.5, 127.1, 127.1, 127.1, 66.9 (CH_2), 48.2 (CH_2), 42.5 (CH_2) MS, m/z (I_r/%): 191 (35) (M^+), 105 (100) (PhCO), 86 (72) (M^+ – PhCO), 77 (75) (Ph), 28 (72) (CO)

Table 2. (continued)

Entry	Characterisation data
29	Phenyl(pyrrolidin-1-yl)methanone Colourless oil IR, $\tilde{\nu}$/cm^{-1}: 3027 (Ph), 2935 (CH_2), 2854 (CH_2), 1633 (C═O) ^{1}H NMR (400 MHz, $CDCl_3$), δ: 7.52–7.51 (m, 2H, Ph), 7.40–7.39 (m, 3H, Ph), 3.65 (m, 2H, CH_2), 3.42 (m, 2H, CH_2), 1.98–1.93 (m, 2H, CH_2), 1.90–1.84 (m, 2H, CH_2) ^{13}C NMR (125 MHz, $CDCl_3$), δ: 170.0 (CO), 139.0, 129.7, 128.2, 127.0, 49.6 (CH_2), 46.1 (CH_2), 26.4 (CH_2), 24.4 (CH_2) MS, m/z (I_r/%): 175 (18) (M^+), 104 (100) (PhCO), 70 (68) (M^+ – PhCO), 28 (100) (CO)
30	*N*-Benzylhexanamide White solid IR, $\tilde{\nu}$/cm^{-1}: 3264 (NH), 3060 (Ph), 3027 (Ph), 2917 (CH_2), 1615 (C═O) ^{1}H NMR (400 MHz, $CDCl_3$), δ: 7.37–7.25 (m, 5H, Ph), 5.69 (brs, 1H, NH) D_2O exchangeable, 4.45 (d, 2H, $^3J_{HH}$ = 5.7 Hz, CH_2), 2.21 (t, 2H, $^3J_{HH}$ = 7.4 Hz, CH_2), 1.66 (p, 2H, $^3J_{HH}$ = 7.5 Hz, CH_2), 1.37–1.24 (m, 4H, CH_2), 0.89 (t, 3H, $^3J_{HH}$ = 6.8 Hz, CH_3) ^{13}C NMR (125 MHz, $CDCl_3$), δ: 173.2 (CO), 138.5, 128.8, 127.9, 127.6, 43.6 (CH_2), 36.9 (CH_2), 31.6 (CH_2), 25.6 (CH_2), 22.5 (CH_2), 14.1 (CH_3) MS, m/z (I_r/%): 205 (6) (M^+), 107 (89) ($PhCH_2NH$), 92 (88) ($PhCH_2$), 45 (89) (CONH), 29 (100) (CO)

Table 3. Optimisation of conditions for CAEA-catalysed transamidation of benzamide with benzylamine

Entry	Molar ratio benzamide/benzylamine	Catalyst content	Solvent	Temperature	Time	Isolated yield
		mole %		℃	h	%
1	1/1.1	0	–	100	5	trace
2	1/1.1	1.61	–	100	5	10
3	1/1.1	1.61	–	110	5	30
4	1/1.1	1.61	–	120	5	50
5	1/1.1	1.61	–	130	5	75
6	1/1.1	1.61	–	140	5	95
7	1/1.1	1.61	–	150	5	60
8	1/1.1	1.61	–	160	5	45
9	1/1.1	1.28	–	140	5	75
10	1/1.1	0.80	–	140	5	50
11	1/1.1	2.57	–	140	5	80
12	1/1.1	3.22	–	140	5	85
13	1/1.1	1.61	H_2O	140	5	0
14	1/1.1	1.61	H_2O/ethylenglycol	140	5	20
15	1/1.1	1.61	ethylenglycol	140	5	60
16	1/1.1	1.61	toluene	140	5	85
17	1/1.0	1.61	–	140	5	90
18	1/1.2	1.61	–	140	5	80
19	1/1.5	1.61	–	140	5	60
20[a]	1/1.1	2.60	–	140	5	30
21[b]	1/1.1	1.56	–	140	5	50
22[c]	1/1.1	1.56	–	140	5	50

a) Reaction was performed in the presence of (*II*); *b*) reaction was performed in the presence of $Ce(NO_3)_3 \cdot 6H_2O$; *c*) reaction was performed in the presence of a mixture of $Ce(NO_3)_3 \cdot 6H_2O$ (1.56 mole %) and ethanolamine (2.50 mole %).

version of transamidation, the reaction was performed at different temperatures and higher conversions were found at 140 ℃. Performing the transamidation reaction at higher temperatures concomitant with the formation of by-products and lower temperatures leads to formation of the desired product in longer reaction times (Table 3, entries 2–8). In order to introduce the same catalyst equivalents in different experiments, the exact amount of the catalyst used was determined on the basis of the loading value in each experiment. The effect of different amounts of catalyst was studied on the reaction rate (Table 3, entries 9–12). The desired product was obtained with a high yield in the presence of 0.01 g (1.61 mole % of CAEA contains 0.002 g, 0.01 mmol, of Ce) of the catalyst. By performing the reaction in the presence of 0.008 g (1.28 mole % of CAEA contains 0.001 g, 0.01 mmol, of Ce) and 0.005 g (0.80 mole % of CAEA contains 0.001 g, 0.007 mmol,

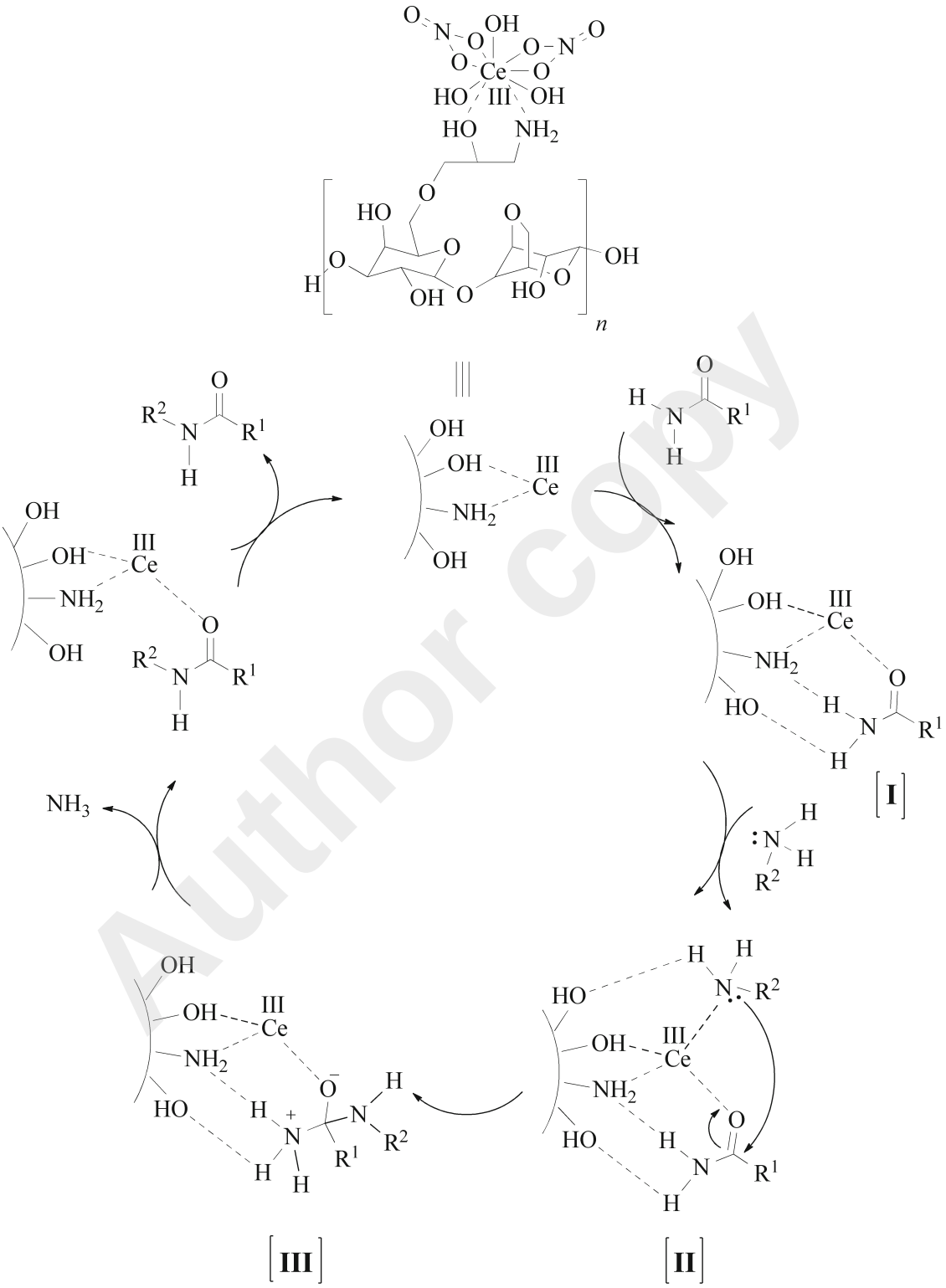

Fig. 3. Proposed mechanism of transamidation of carboxamides in the presence of Ce(III) immobilised on aminated epichlorohydrin-activated agarose matrix (CAEA).

of Ce) of the catalyst, the transamidation reaction proceeded with only 75 % and 50 % yields after 5 h (Table 3, entries 9 and 10). When the transamidation reaction was carried out in the presence of additional amounts of the catalyst (0.01 g, 2.57 mole %, of CAEA and 0.02 g, 3.22 mole %, of CAEA), the formation of by-products reduced the conversion of reactants to the desired product (Table 3, entries 11 and 12). In order to investigate the effect of different solvents, the transamidation reaction of benzamide with

benzylamine was carried out in polar solvents such as: H_2O, H_2O/ethylene glycol ($\varphi_r = 50 : 50$), ethylene glycol, and toluene (Table 3, entries 13–16). It was found that the best conversion was obtained under solvent-free conditions. By considering the results from Table 3, applying a 1/1.1 molar ratio of benzamide/benzylamine produced *N*-benzylbenzamide with a high yield without the formation of any by-products (Table 3, compare entry 6 with entries 17–19). In order to ascertain the major role played by CAEA as a catalyst in the transamidation reaction and by applying the optimal reaction conditions, two further reactions between benzamide and benzylamine were performed. The first reaction was performed in the presence of aminated epichlorohydrin-activated agarose matrix (*II*) (0.01 g, 2.60 mole %) and the second was carried out in the presence of $Ce(NO_3)_3 \cdot 6H_2O$. After an appropriate reaction time (5 h), the extent of former reaction was 30 % and that of the latter one, by applying 0.006 g, 1.56 mole %, of $Ce(NO_3)_3 \cdot 6H_2O$, was 50 % with the formation of by-products (Table 3, entries 20 and 21). The result from entry 20 shows the catalytic activity of the aminated epichlorohydrin-activated agarose matrix (*II*) in the transamidation reaction. This activity which preceded the transamidation reaction to some extent is the result of the formation of hydrogen bonding between OH and NH_2 of (*II*) with carboxamide and amine in the reaction mixture (see Fig. 3). To better understand the catalytic activity of CAEA, the reaction was carried out with a mixture of $Ce(NO_3)_3 \cdot 6H_2O$ (1.56 mole %) and ethanolamine (2.50 mole %). The desired product was obtained with a 50 % yield after 5 h (Table 3, entry 22). This result leads to the conclusion that the immobilisation of Ce(III) on an aminated epichlorohydrin-activated agarose matrix (*II*) improved the catalytic activity of Ce(III) in the transamidation reaction.

The transamidation reaction of different carboxamides with various aliphatic and aromatic amines was studied on the basis of the optimised reaction conditions, 0.01 g of the catalyst (containing 0.002 g, 0.01 mmol, of Ce) at 140 ℃ under solvent-free conditions and to show the general application and versatility of the present protocol. The results are summarised in Table 4. Because of the importance of secondary amides in synthetic and biological polymers, attention was focused on the synthesis of this class of substrates resulting from the current transamidatiom reaction. The transamidation reactions of benzamide and substituted benzamide were performed smoothly with benzylamine to deliver the corresponding secondary amides (Table 4, entries 1–9). Benzamides substituted with electron-withdrawing groups at *para*-position considerably enhanced the product yields (Table 4, entries 8 and 9). Halogen-substituted benzamide also performed well in the reactions (Table 4, entries 5–7). As regards the steric effects, benzamides having *ortho* substituent afforded the desired products with longer reaction times (compare entries 6 and 7). Comparatively, electron-donating substituents prolonged the transamidation reactions of benzamides (Table 4, entries 2–4).

The transamidation of isonicotinamide with benzylamine afforded its *N*-benzylated analogue, providing convenient access to this class of pharmaceutically important compounds (Table 4, entry 10). From the results obtained from Table 4 and on the basis of the proposed mechanism in Fig. 3, the electrophilicity of the carbonyl group of amides is thought to play an essential role in the reaction rate. The present system was further examined for the transamidation of aliphatic amides (Table 4, entries 11–16 and 30). The transamidation of aliphatic amides with benzyl amine afforded their *N*-substituted analogues with good yields but over a long period of time. The generality of this CAEA-catalysed transamidation was further demonstrated in the reaction of benzamide with a variety of aliphatic (primary and secondary) and aromatic amines (Table 4, entries 19–29). Electron-releasing groups on substituted benzyl amines accelerate the reaction, as expected due to its increased nucleophilicity (Table 4, entries 17). By contrast, the *ortho*-halogenated benzyl amine with lower nucleophilicity, possibly caused by the steric hindrance and inductive effects of halogene, reacts slower than benzylamine (Table 4, entry 18). With the methodology thus developed, attention turned to the transamidation of benzamide with aromatic amines under the standardised conditions (Table 4, entries 19–22). The reaction was rapid with electron-rich aniline and was completed within 3 h affording a 90 % yield, but when benzamide was treated with aniline the product was obtained after 11 h with a 20 % yield (Table 4, entries 19–22). Benzamide was also treated with furan-2-ylmethylamine (Table 4, entry 23). The transamidation reaction was completed within 8 h giving a 92 % yield (Table 4, entry 23). Following these promising results, attention was directed to the reaction of benzamide with primary and secondary aliphatic amines such as: cyclohexylamine, butan-1-amine, 3-ethoxypropylamine, piperidine, morpholine and pyrrolidine. In all cases, the reaction was smooth, giving the corresponding *N*-substituted benzamides and the yield ranged from 85 % to 95 % (Table 4, entries 24–29).

Mechanism of the present catalytic transamidation requires elucidation, thus, the following mechanism may be proposed for the catalytic transamidation of carboxamides with amines in the presence of CAEA (Fig. 3).

It may be seen that the transamidation reaction is the activation of the electrophile (carboxamide) via coordination to Ce(III) which subsequently generates structure **I** (Fig. 3). On the other hand, the amine was activated by coordination of Ce(III) and also by the formation of hydrogen bonding with hydroxy groups on the surface of catalyst. These interactions between

Table 4. Transamidation reactions of various carboxamides and amines in the presence of CAEA (Fig. 2)

Compound	R^1	R^2	Time	Isolated yield	M.p.	Reference
			h	%	℃	
1	Ph	$PhCH_2$	5	95	101–102 (100–103)	Iranpoor et al. (2013)
2	4-$MeOC_6H_4$	$PhCH_2$	8	60	119–120 (118–122)	Iranpoor et al. (2013)
3	3,5-$Me_2C_6H_3$	$PhCH_2$	15	70	105–107 (107–108)	Kunishima et al. (2004)
4	4-MeC_6H_4	$PhCH_2$	13	85	130–132 (129–132)	Iranpoor et al. (2013)
5	4-BrC_6H_4	$PhCH_2$	6	60	167–168 (168)	Kawagoe et al. (2013)
6	2-ClC_6H_4	$PhCH_2$	9	70	160–162 (161–163)	Tang and Chen (2012)
7	3,4-$Cl_2C_6H_3$	$PhCH_2$	4	80	103–105 (105–106)	Wang et al. (2014b)
8	3-$NO_2C_6H_4$	$PhCH_2$	4	90	94–96 (95)	Fang et al. (2008)
9	4-$NO_2C_6H_4$	$PhCH_2$	3	95	138–140 (140)	Kawagoe et al. (2013)
10	pyridyl	$PhCH_2$	8	95	81–82 (81–83)	Ghodsinia et al. (2013)
11	(*E*)-PhCH=CH	$PhCH_2$	16	30	134–137 (136–139)	Iranpoor et al. (2013)
12	4-ClPhCH=CH	$PhCH_2$	13	35	149–151 (150–151)	Kawagoe et al. (2013)
13	3-NO_2PhCH=CH	$PhCH_2$	9	70	184–186 (185–186)	Starkov and Sheppard (2011)
14	2,4-$Cl_2C_6H_3OCH_2$	$PhCH_2$	11	45	oil	Yamansarova et al. (2005)
15	$(Ph)_2CH$	$PhCH_2$	22	80	126–128 (127–128)	Lanigan et al. (2013)
16	$CH_3(CH_2)_7CH{=}CH(CH_2)_6CH_2$	$PhCH_2$	25	90	oil	Ruiz-Méndez et al. (2001)
17	Ph	4-$MeOC_6H_4CH_2$	2	90	83–85 (82–85)	Iranpoor et al. (2013)
18	Ph	2-$ClC_6H_4CH_2$	6	80	106–108 (107–108)	Wang et al. (2014b)
19	Ph	C_6H_5	11	20	158–160 (160–162)	Iranpoor et al. (2013)
20	Ph	4-$MeOC_6H_4$	4	60	163–165 (164–165)	Quan et al. (2014)
21	Ph	3,4-$Me_2C_6H_3$	5	50	147–149 (148–150)	Du et al. (2014)
22	Ph	4-MeC_6H_4	9	60	156–158 (157–159)	Guo et al. (2013)
23	Ph	furan-2-ylmethyl	8	92	96–98 (98–99)	Wang et al. (2014b)
24	Ph	cyclohexyl	12	90	149–151 (150–152)	Rossi et al. (2013)
25	Ph	butyl	10	85	39–41 (37–38)	Wang et al. (2014b)
26	Ph	3-ethoxypropyl	14	80	oil	present study
27	Ph	piperidine	15	95	oil	Schley et al. (2011)
28	Ph	morpholine	10	90	oil	Zhu et al. (2011)
29	Ph	pyrrolidine	16	95	oil	Zhu et al. (2011)
30	$CH_3(CH_2)_4$	$PhCH_2$	4	95	49–51 (50–52)	Dam et al. (2010)

Table 5. Transamidation of benzamide with benzylamine in the presence of 0.01 g of reused CAEA

Entry	Run	Time	Isolated yield
		h	%
1	1[a]	5	95
2	2	5	95
3	3	5	95
4	4	5	95
5	5	5	95
6	6[b]	5	85

a) Reaction was performed in the presence of 0.01 g, 1.61 mole %, of CAEA (contains 0.002 g, 0.01 mmol, of Ce); *b*) reaction was performed in the presence of 0.01 g, 0.70 mole %, of CAEA (contains 0.0009 g, 0.006 mmol, of Ce).

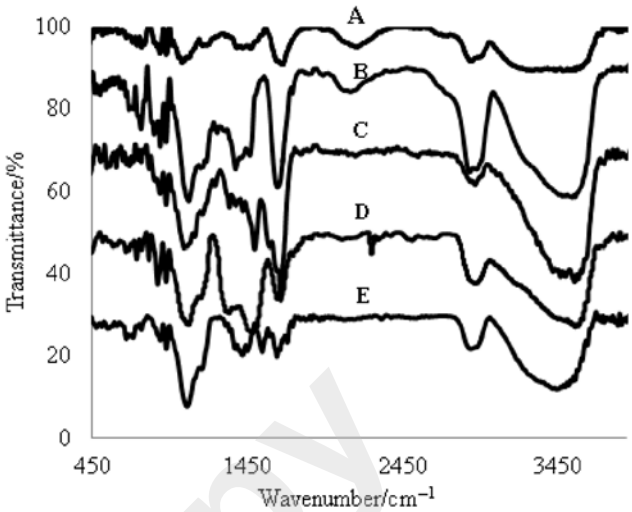

Fig. 4. FT-IR spectra of washed agarose (A), epoxy-activated agarose matrix (B), aminated epichlorohydrin-activated agarose matrix (C), Ce(III) immobilised on aminated epichlorohydrin-activated agarose matrix (D), and reused Ce(III) immobilised on aminated epichlorohydrin-activated agarose matrix (E).

the two reactants (amide and amine) with CAEA place them close together and lead to the formation of structure **II**. Then, the facilitated nucleophilic attack of amine on the amide carbonyl group leads to the formation of structure **III**. The cleavage of **III** leads to the rapid extrusion of ammonia and the release of *N*-alkylated amide. The catalyst re-enters the catalytic cycle by making the active sites available for further use. Further investigations into the mechanism and scope of this reaction are currently underway.

A significant feature of this environmentally benign and cost-effective straightforward protocol for the transamidation of carboxamides with amines is its reusability. Recovery of the CAEA in the reaction of benzamide with benzylamine was achieved by centrifugation and washing with ethyl acetate and acetone several times to remove all organic compounds, and then drying at ambient temperature. Table 5 shows the results obtained after six cycles. On the basis of the results obtained, the efficiency of the catalyst in the transamidation reaction remained after five cycles. Inductively coupled plasma (ICP) analysis shows that freshly prepared CAEA contains 0.22 g, 1.61 mmol, of Ce per 1 g of CAEA, while after the 6th re-use the CAEA contains 0.09 g, 0.70 mmol, of Ce per 1 g of CAEA. In other words, during the recovery process of the catalyst, the catalytic activity maintained its effectivity after six reuses of CAEA. No significant loss of activity of the catalyst was observed, despite some leaching of Ce(III) during the recovery process of the catalyst. Also, the FT-IR spectrum of the 6th reused CAEA (Fig. 4, spectrum E) in comparison with the freshly prepared CAEA shows that the intensities of absorption bands (Ce—N and Ce—O frequencies) decreased to a small extent.

Characterisation of catalyst

The catalyst structure was defined by FT-IR spectroscopy. Fig. 4 illustrates the FT-IR spectra of washed agarose, the epoxy-activated agarose matrix, the aminated epichlorohydrin-activated agarose matrix (*II*) and Ce(III) immobilised on aminated epichlorohydrin-activated agarose matrix (CAEA).

The principal bands for agarose were observed at 3553 cm^{-1} (O—H stretching), 2893 cm^{-1} (CH_2), 1655 cm^{-1} (H—O—H) attributed to the stretching vibration of water bound to polysaccharide, 1082 cm^{-1} and 1035 cm^{-1} (attributed to anti-symmetric stretching vibrations of the C—O—C bridge), 929 cm^{-1} (characteristic of 3,6-anhydrogalactose), and 889 cm^{-1} (attributed to the C—H angular deformation of β anomeric carbon) (Jegan et al., 2011). An absorption band at 1256 cm^{-1} due to the epoxy ring of the epichlorohydrin-activated agarose matrix. The appearance of two absorption bands at 3560 cm^{-1} and 3472 cm^{-1} attributed to –NH_2 stretching frequencies and also two other absorption bands at 1593 cm^{-1} and 1245 cm^{-1} due to N—H bending vibration and C—N stretching vibrations confirmed the ring-opening of the epoxy ring with ammonia. The coordination of the aminated epichlorohydrin-activated agarose matrix by Ce(III) was corroborated by the absorption bands at 588 cm^{-1}, 539 cm^{-1}, and 476 cm^{-1}, 421cm^{-1} (which is attributed to Ce—N and Ce—O stretching vibrations) in the FT-IR spectrum of CAEA. Moreover, the far IR spectrum of CAEA (Fig. 5) exhibited not only the above-mentioned absorption bands but also other bands at 597 cm^{-1}, 568 cm^{-1} (Ce—N), and 426 cm^{-1} (Ce—O) which confirmed the immobilisation of Ce(III) on the support framework. The coordination of nitrogen by Ce(III) was also established by the appearance of the absorption bands of –NH_2 and C—N at a lower frequency (3542 cm^{-1}, 3458 cm^{-1}, and 1190 cm^{-1}, respectively) than the un-

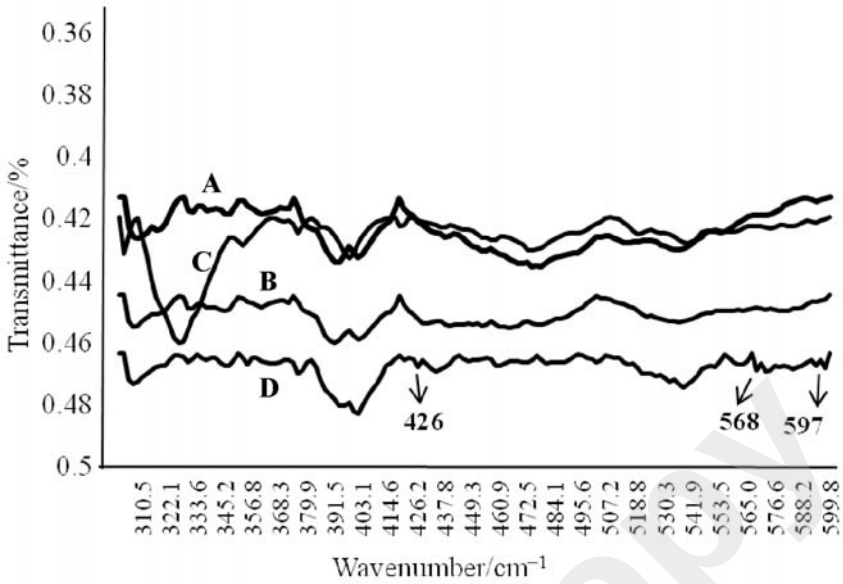

Fig. 5. Far IR spectra of washed agarose (A), epoxy-activated agarose matrix (B), aminated epichlorohydrin-activated agarose matrix (C), and Ce(III) immobilised on aminated epichlorohydrin-activated agarose matrix (D).

coordinated ligand form (*II*). The characteristic frequencies of the coordinated nitrate groups of CAEA are 1744 cm^{-1} (which did not exist in the FT-IR spectrum of the aminated epichlorohydrin-activated agarose matrix (*II*) due to the nitrate stretching vibration), 1487 cm^{-1}(due to the N═O vibration) which was overlapped by the C—H bending vibration frequency of the aminated epichlorohydrin-activated agarose matrix (*II*), and 1326 cm^{-1} (which suggest that nitrate anions as bidentate ligands in CAEA are covalently bonded and are present inside the coordination sphere). Another broad absorption band at 1376 cm^{-1} due to the ionic nitrate is also present in the spectra (Gaye et al., 2003).

Thermogravimetric studies of the washed agarose, the epoxy-activated agarose matrix (*I*), the aminated epichlorohydrin-activated agarose matrix (*II*), Ce(III) immobilised on aminated epichlorohydrin-activated agarose matrix (CAEA) at a heating rate of 10 ℃ min^{-1} are shown in Figs. 6–9.

Three regions of mass loss are observed in the TGA curve of the washed agarose. The first stage of degradation represents the loss of the physically adsorbed and hydrogen-bonded water (mass loss 10.0 %, from 22–180 ℃). The major mass loss took place in the second step (mass loss 76.0 %, 180–420 ℃) and was followed by a further mass loss in the third step (97.0 %, 420–514 ℃). The second stage represents some chain scission of washed agarose. In the third stage, complete decomposition of the agarose main chains occurred (Arnaouty et al., 2009; Anirudhan et al., 2012).

Similarly, the TGA thermogram of the epoxy-activated agarose matrix (*I*) exhibited three distinct mass loss stages. As the introduction of the epoxy ring to the main chain of the agarose decreases the hydrophilicity of agarose, every stage of the mass loss occurred at a lower temperature than in the case of

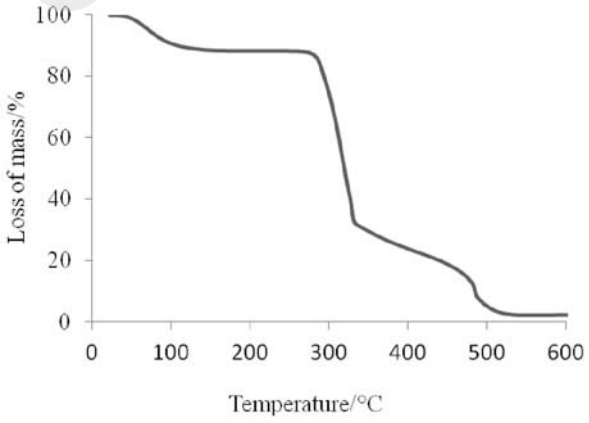

Fig. 6. TGA thermogram of washed agarose.

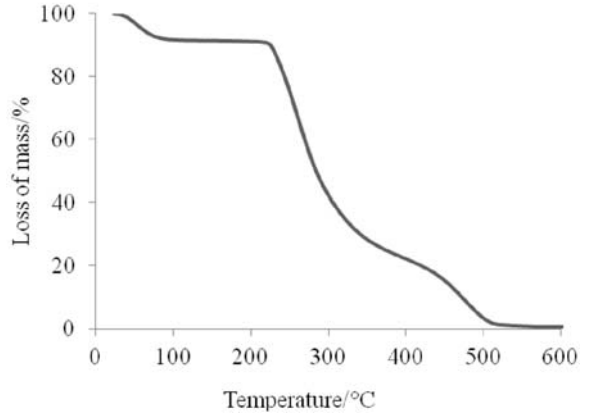

Fig. 7. TGA thermogram of epoxy-activated agarose (*I*).

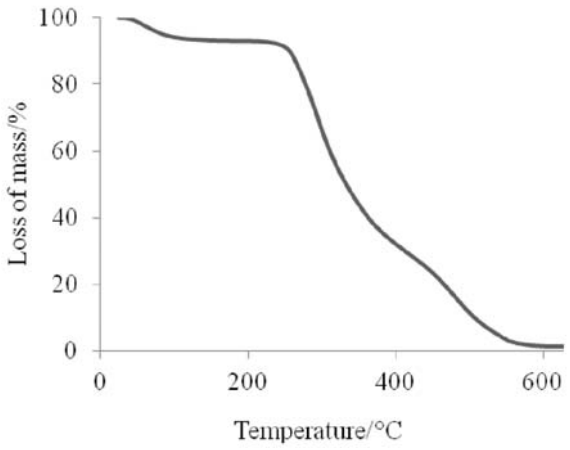

Fig. 8. TGA thermogram of aminated epichlorohdrin-activated agarose matrix (*II*).

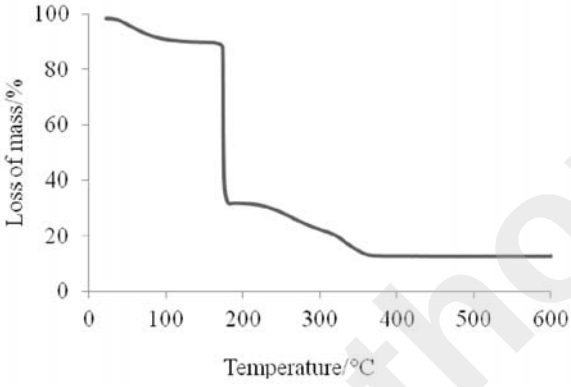

Fig. 9. TGA thermogram of Ce(III) immobilised on aminated epichlorohydrin-activated agarose matrix (*III*).

the washed agarose. As can be seen, water elimination occurred at the first step (mass loss 8.0 %, from 23–153 ℃). The second stage (mass loss 78.0 %, from 153–400 ℃) can be attributed to the decomposition of the epoxy ring and chemical degradation of some C—C bonds of the agarose backbone. Because of the existence of the epoxy ring, the third stage (mass loss 97 %, 400–620 ℃) which corresponds to the complete decomposition of the epoxy- activated agarose matrix (*I*) began at a lower temperature than in the case of the washed agarose. Surprisingly, chemical degradation of (*I*) extended to a higher temperature than with the washed agarose (Oza et al., 2012).

The TGA thermogram of the aminated epichlorohydrin-activated agarose matrix (*II*) exhibited a three-stage degradation pattern. Each stage of the mass loss occurred at a higher temperature than with (*I*) and the washed agarose. This confirmed the modification of (*I*) by the ring-opening of the epoxy ring with ammonia which increased the thermal stability of the polysaccharide. The first step (mass loss 12.0 %, 24–198 ℃) may be attributed to evaporation of the moisture and the easily degraded components which are strongly bonded to the polysaccaride chain via hydrogen-bonding with the immobilised NH_2 group on the polymer chain. Water elimination also occurred at a higher temperature than with (*I*) and the washed agarose. The evolution of ammonia and partial degradation of the polysaccharide chain occurred in the second stage (mass loss 74.0 %, 198–442 ℃) as the major mass loss in the thermogravimetric analysis of (*II*). The third stage of mass loss (98.0 %, 442–594 ℃) was predominantly the characteristic complete degradation of the polysaccharide structure (breaking down and cracking of the main chain).

By considering the TGA thermogram of the aminated epichlorohydrin-activated agarose matrix (*II*) and the elemental analysis data which are in good agreement with each other, it was clear that 1.0 g of the aminated epichlorohydri-activated agarose matrix (*II*) contains 0.0056 g, 0.4 mmol, of nitrogen (Fig. 8).

The TGA thermogram of CAEA with three steps of mass loss differs from the previous samples. As the hydrogen-bonding was decreased to some extent by the coordination of $–NH_2$ and –OH by Ce(III), removal of the moisture and hydrogen-bonded water (mass loss 8.0 %, 22–125 ℃) occurred within a narrow temperature range. The second stage (mass loss 77.0 %, 125–292 ℃) represents the exit of the water coordinated by Ce(III) and degradation of the cerium complex from 140 ℃ to 290 ℃. Nitrate was also removed in the second stage (Zahir, 2013). In the third stage (mass loss 85.0 %, 292–480 ℃), the complete degradation of the polysaccharide chain occurred and the char yield (15 %) corresponds to the remaining cerium which was converted to CeO_2 above 600 ℃ (Alghool et al., 2013).

The cerium content of CAEA as obtained by inductively coupled plasma (ICP) analysis was 0.22 g, 1.61 mmol of Ce per 1.0 g of CAEA.

Agarose has a broad amorphous region in its natural structure, as indicated by its X-ray diffraction pattern (Raphael et al., 2010). Fig. 10 shows the XRD patterns for CAEA. One peak can be observed between 40° and 80° in the diffractogram, which indicates a low amount of the cerium oxide crystal structure (Silveira et al., 2012) while no such peaks are visible in the XRD of pure agarose between 40° and 80°. A broad band centred at about $2\theta = 20°$ confirms the amorphous character of CAEA.

Conclusions

In conclusion, agarose was applied as a non-toxic, low-cost, degradable natural support for the entrapment and ligation with Ce(III) and a novel method of the transamidation of carboxamides with aliphatic, aromatic, cyclic, acyclic, primary, and secondary amines was developed using catalytic amounts of CAEA as a "green" and effective catalyst under

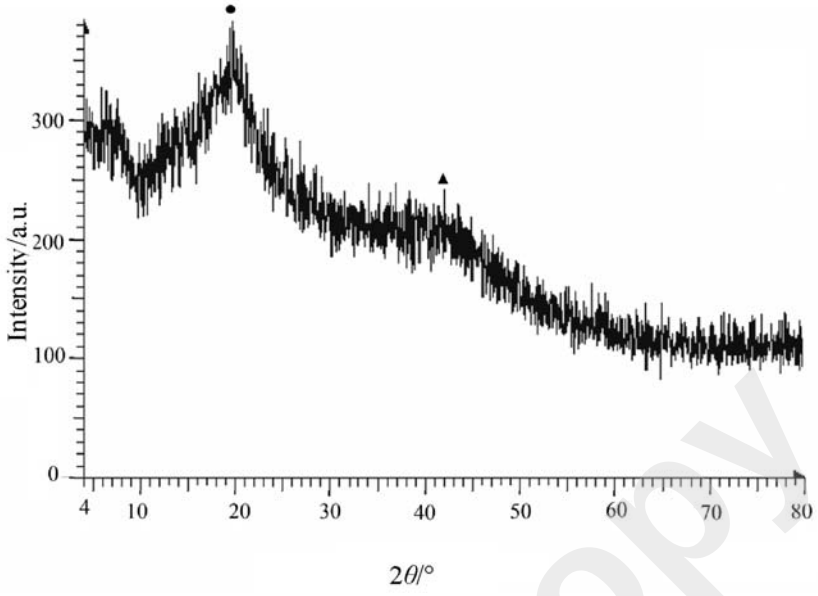

Fig. 10. XRD pattern of Ce(III) immobilised on aminated epichlorohydrin-activated agarose matrix (*III*): agarose (●), CeO_2 (▲).

solvent-free conditions. The catalyst is recyclable and provides a wide range of amides. In view of the economic attractiveness and the operational simplicity of CAEA, the procedure which proceeds smoothly and can tolerate a number of functionalities is proposed as being of important synthetic value for access to a variety of *N*-alkylated amides.

Supplementary information

The supplementary data associated with this article can be found in the online version of this paper (DOI: 10.1515/chempap-2015-0168).

Acknowledgements. The authors gratefully acknowledge the partial support afforded to this study by Ferdowsi University of Mashhad Research Council (grant no. p/3/29781).

References

Alghool, S., Abd El-Halim, H. F., Abd El-sadek, M. S., Yahia, I. S., & Wahab, L. A. (2013). Synthesis, thermal characterization, and antimicrobial activity of lanthanum, cerium, and thorium complexes of amino acid Schiff base ligand. *Journal of Thermal Analysis and Calorimetry*, *112*, 671–681. DOI: 10.1007/s10973-012-2628-4.

Allen, C. L., Atkinson, B. N., & Williams, J. M. J. (2012). Transamidation of primary amides with amines using hydroxylamine hydrochloride as an inorganic catalyst. *Angewandte Chemie International Edition*, *51*, 1383–1386. DOI: 10.1002/anie.201107348.

Anirudhan, T. S., Rauf, T. A., & Rejeena, S. R. (2012). Removal and recovery of phosphate ions from aqueous solutions by amine functionalized epichlorohydrin-grafted cellulose. *Desalination*, *285*, 277–284. DOI: 10.1016/j.desal.2011.10.014.

Atkinson, B. N., Chhatwal, A. R., Lomax, H. V., Walton, J. W., & Williams, J. M. J. (2012). Transamidation of primary amides with amines catalyzed by zirconocene dichloride. *Chemical Communications*, *48*, 11626–11628. DOI: 10.1039/c2cc37427g.

Ayub Ali, Md., Hakim Siddiki, S. M. A., Kon, K., & Shimizu, K. i. (2014). Fe^{+3}-exchanged clay catalyzed transamidation of amides with amines under solvent-free condition. *Tetrahedron Letters*, *55*, 1316–1319. DOI: 10.1016/j.tetlet.2013.12.111.

Becerra-Figueroa, L., Ojeda-Porras, A., & Gamba-Sánchez, D. (2014). Transamidation of carboxamides catalyzed by Fe(III) and water. *The Journal of Organic Chemistry*, *79*, 4544–4552. DOI: 10.1021/jo500562w.

Cao, X. J., Zhu, J. W., Wang, D. W., Dai, G. C., & Wu, X. Y. (1997). Affinity chromatography purification of urokinase with epichlorohydrin activited agarose martix. *Chinese Journal of Chemical Enginneering*, *5*, 69–73.

Dam, J. H., Osztrovszky, G., Nordstrøm, L. U., & Madsen, R. (2010). Amide synthesis from alcohols and amines catalyzed by ruthenium *N*-heterocyclic carbene complexes. *Chemistry - A European Journal*, *16*, 6820–6827. DOI: 10.1002/chem.201000569.

Du, J. A., Luo, K., & Zhang, X. L. (2014). Synthesis of amides through an oxidative amidation of tetrazoles with aldehydes under transition-metal-free conditions. *RSC Advances*, *4*, 54539–54546. DOI: 10.1039/c4ra07658c.

El-Arnaouty, M. B., Eid, M., Atia, A., & Dessouki, A. (2009). Characterization and application of grafted polypropylene and polystyrene treated with epichlorohydrin coupled with cellulose or starch for immobilization processes. *Journal of Applied Polymer Science*, *112*, 629–638. DOI: 10.1002/app.29364.

Fang, C., Qian, W. X., & Bao, W. L. (2008). A mild and clean method for oxidative formation of amides from aldehydes and amines. *Synlett*, *2008*, 2529–2531. DOI: 10.1055/s-2008-1078218.

Fu, R. Z., Yang, Y., Chen, Z. K., Lai, W. C., Ma, Y. F., Wang, Q., & Yuan, R. X. (2014). Microwave-assisted heteropolyanion-based ionic liquids catalyzed transamidation of non-activated carboxamides with amines under solvent-free conditions. *Tetrahedron*, *70*, 9492–9499. DOI: 10.1016/j.tet.2014.10.066.

Gaye, M., Tamboura, F. B., & Sall, A. S. (2003). Spectroscopic studies of some lanthanide(III) nitrate complexes synthesized from a new ligand 2,6-bis-(salicylaldehyde hydrazone)-

4-chlorophenol. *Bulletin of the Chemical Society of Ethiopia*, *17*, 27–34. DOI: 10.4314/bcse.v17i1.61726.

Ghodsinia, S. S. E., Akhlaghinia, B., Safaei, E., & Eshghi, H. (2013). Green and selective synthesis of *N*-substitued amides using water soluble porphyrazinato copper(II) catalyst. *Journal of the Brazilian Chemical Society, 24*, 895–903. DOI: 10.5935/0103-5053.20130115.

Ghosh, S. C., Li, C. C., Zeng, H. C., Ngiam, J. S. Y., Seayad, A. M., & Chen, A. Q. (2014). Mesoporous niobium oxide spheres as an effective catalyst for the transamidation of primary amides with amines. *Advanced Synthesis & Catalysis*, *356*, 475–484. DOI: 10.1002/adsc.201300717.

Guo, Z. Q., Liu, Q., Wei, X. H., Zhang, Y. B., Tong, H. B., Chao, J. B., Guo, J. P., & Liu, D. S. (2013). 2-Aminopyrrolyl dilithium compounds: Synthesis, structural diversity, and catalytic activity for amidation of aldehydes with amines. *Organometallics*, *32*, 4677–4683. DOI: 10.1021/om4006609.

Hoerter, J. M., Otte, K. M., Gellman, S. H., Cui, Q. A., & Stahl, S. S. (2008). Discovery and mechanistic study of AlIII-catalyzed transamidation of tertiary amides. *Journal of the American Chemical Society*, *130*, 647–654. DOI: 10.1021/ja0762994.

Iranpoor, N., Firouzabadi, H., Motevalli, S., & Talebi, M. (2013). Palladium-free aminocarbonylation of aryl, benzyl, and styryl iodides and bromides by amines using Mo(CO)6 and norbornadiene. *Tetrahedron*, *69*, 418–426. DOI: 10.1016/j.tet.2012.10.002.

Jegan, A., Ramasubbu, A., Saravanan, S., & Vasanthkumar, S. (2011). One-pot synthesis and characterization of biopolymer-iron oxide nanocomposite. *International Journal of Nano Dimension*, *2*, 105–110.

Kawagoe, Y., Moriyama, K., & Togo, H. (2013). Facile preparation of amides from carboxylic acids and amines with ion-supported Ph_3P. *Tetrahedron*, *69*, 3971–3977. DOI: 10.1016/j.tet.2013.03.021.

Kunishima, M., Watanaba, Y., Terao, K., & Tani, S. (2004). Substrate-specific amidation of carboxylic acids in a liquid–liquid two phase system using cyclodextrins as inverse phase-transfer catalysts. *European Journal of Organic Chemistry*, *2004*, 4535–4540. DOI: 10.1002/ejoc.200400470.

Lanigan, R. M., Starkov, P., & Sheppard, T. D. (2013). Direct synthesis of amides from carboxylic acids and amines using $B(OCH_2CF_3)_3$. *The Journal of Organic Chemistry*, *78*, 4512–4523. DOI: 10.1021/jo400509n.

Lundberg, H., Tinnis, F., Selander, N., & Adolfsson, H. (2014). Catalytic amide formation from non-activated carboxylic acids and amines. *Chemical Society Reviews*, *43*, 2714–2742. DOI: 10.1039/c3cs60345h.

Oza, M., Meena, R., & Siddhanta, A. K. (2012). Facile synthesis of fluorescent polysaccharides: Cytosine grafted agarose and κ-carrageenan. *Carbohydrate Polymers*, *87*, 1971–1979. DOI: 10.1016/j.carbpol.2011.10.004.

Quan, Z. J., Xia, H. D., Zhang, Z., Da, Y. X., & Wang, X. C. (2014). Ligand-free CuTC-catalyzed *N*-arylation of amides, anilines and 4-aminoantipyrine: synthesis of *N*-arylacrylamides, 4-amido-*N*-phenylbenzamides and 4-amino (*N*-phenyl)antipyrenes. *Applied Organometallic Chemistry*, *28*, 81–85. DOI: 10.1002/aoc.3080.

Rao, S. N., Mohan, R. D., & Adimurthy, S. (2013). L-proline: An efficient catalyst for transamidation of carboxamides with amines. *Organic Letters*, *15*, 1496–1499. DOI: 10.1021/ol4002625.

Raphael, E., Avellaneda, C. O., Manzolli, B., & Pawlicka, A. (2010). Agar-based films for application as polymer electrolytes. *Electrochimica Acta*, *55*, 1455–1459. DOI: 10.1016/j.electacta.2009.06.010.

Rasheed, S., Rao, D. N., Reddy, A. S., Shankar, R., & Das, P. (2015). Sulphuric acid immobilized on silica gel (H_2SO_4–SiO_2) as an eco-friendly catalyst for transamidation. *RSC Advances*, *5*, 10567–10574. DOI: 10.1039/c4ra16571c.

Razavi, N., & Akhlaghinia, B. (2015). Cu(II) immobilized on aminated epichlorohydrin activated silica (CAES): as a new, green and efficient nanocatalyst for preparation of 5-substituted-1*H*-tetrazoles. *RSC Advances*, *5*, 12372–12381. DOI: 10.1039/c4ra15148h.

Rhim, J. W. (2012). Physical-mechanical properties of agar/κ-carrageenan blend film and derived clay nanocomposite film. *Journal of Food Science*, *77*, N66–N73. DOI: 10.1111/j.1750-3841.2012.02988.x.

Rossi, S. A., Shimkin, K. W., Xu, Q., Mori-Quiroz, L. M., & Watson, D. A. (2013). Selective formation of secondary amides via the copper-catalyzed cross-coupling of alkylboronic acids with primary amides. *Organic Letters*, *15*, 2314–2317. DOI: 10.1021/ol401004r.

Ruiz-Méndez, M. V., Posada de la Paz, M., Abian, J., Calaf, R. E., Blount, B., Castro-Molero, N., Philen, R., & Gelpí, E. (2001). Storage time and deodorization temperature influence the formation of aniline-derived compounds in denatured rapeseed oils. *Food and Chemical Toxicology, 39*, 91–96. DOI: 10.1016/s0278-6915(00)00111-3.

Sergeeva, M. V., Mozhaev, V. V., Rich, J. O., & Khmelnitsky, Y. L. (2000). Lipase-catalyzed transamidation of non-activated amides in organic solvent. *Biotechnology Letters*, *22*, 1419–1422. DOI: 10.1023/a:1005621117392.

Schley, N. D., Dobereiner, G. E., & Crabtree, R. H. (2011). Oxidative synthesis of amides and pyrroles via dehydrogenative alcohol oxidation by ruthenium diphosphine diamine complexes. *Organometallics*, *30*, 4174–4179. DOI: 10.1021/om2004755.

Silveira, G., de Morais, A., Mendes Villis, P. C., Marchetti Maroneze, C., Gushikem, Y., Serpa Lucho, A. M., & Pissettia, F. L. (2012). Electrooxidation of nitrite on a silica–cerium mixed oxide carbon paste electrode. *Journal of Colloid and Interface Science*, *369*, 302–308. DOI**:** 10.1016/j.jcis.2011.11.060.

Singh, D. P., Allam, B. K., Singh, K. M., & Singh, V. P. (2014). A binuclear Mn(II) complex as an efficient catalyst for transamidation of carboxamides with amines. *RSC Advances*, *4*, 1155–1158. DOI**:** 10.1039/c3ra45176c.

Starkov, P., & Sheppard, T. D. (2011). Borate esters as conveninet reagents for direct amidation of carboxylic acids and transamidation of primary amides. *Organic & Biomolecular Chemistry, 9*, 1320–1323. DOI: 10.1039/c0ob01069c.

Stephenson, N. A., Zhu, J. A., Gellman, S. H., & Stahl, S. S. (2009). Catalytic transamidation reactions compatible with tertiary amide metathesis under ambient conditions. *Journal of the American Chemical Society, 131*, 10003–10008. DOI: 10.1021/ja8094262.

Tamura, M., Tonomura, T., Shimizu, K. i., & Satsuma, A. (2012). Transamidation of amides with amines under solvent-free conditions using a CeO_2 catalyst. *Green Chemistry*, *14*, 717–724. DOI: 10.1039/c2gc16316k.

Tang, X. R., Chen, S. L., & Wang, L. (2012). Optimization and antifungal activity of chalcone analogues. *Asian Journal of Chemistry*, *24*, 2516–2518.

Wang, N. N., Zou, X. Y., Ma, J. A., & Li, F. (2014a). The direct synthesis of *N*-alkylated amides *via* a tandem hydration/*N*-alkylation reaction from nitriles, aldoximes and alcohols. *Chemical Communications, 50*, 8303–8305. DOI: 10.1039/c4cc02742f.

Wang, Y. H., Wang, F., Zhang, C. F., Zhang, J. A., Li, M. R., & Xu, J. (2014b). Transformylating amine with DMF to formamide over CeO_2 catalyst. *Chemical Communication*s, *50*, 2438–2441. DOI: 10.1039/c3cc48400a.

Wu, Y., Geng, F. Y., Chang, P. R., Yu, J. G., & Ma, X. F. (2009). Effect of agarose on the microstructure and perfor-

mance of potato starch film. *Carbohydrate Polymers*, *76*, 299–304. DOI: 10.1016/j.carbpol.2008.10.031.

Yamansarova, E. T., Kukovinets, O. S., Zainullin, R. A., Galin, F. Z., & Abdullin, M. I. (2005). Synthesis of nitrogen-containing phenoxyacetic acid derivatives. *Russian Journal of Organic Chemistry, 41*, 546–550. DOI: 10.1007/s11178-005-0201-3.

Zahir, M. H. (2013). Synthesis and characterization of trivalent cerium complexes of p-tert-butylcalix[4,6,8]arenes: Effect of organic solvents. *Journal of Chemistry*, *2013*, 494392. DOI: 10.1155/2013/494392.

Zhang, M., Imm, S., Bähn, S., Neubert, L., Neumann, H., & Beller, M. (2012). Efficient copper(II) catalyzed transamidation of non-activated primary carboxamides and ureas with amines. *Angewandte Chemie International Edition*, *51*, 3905–3909. DOI: 10.1002/anie.201108599.

Zhu, Y. H., Li, C. Z., Biying, A. O., Sudarmadji, M., Chen, A. G., Tuan, T. D., & Seayad, A. M. (2011). Stabilized well-dispersed Pd(0) nanoparticles for aminocarbonylation of aryl halides. *Dalton Transactions, 40*, 9320–9325. DOI: 10.1039/c1dt10927h.